Theory for the spin caloritronic nano-oscillator

S. M. Rezende[1,*] and R. L. Rodríguez-Suárez[2]
[1]*Departamento de Física, Universidade Federal de Pernambuco, 50670-901 Recife, PE, Brazil*
[2]*Facultad de Física, Pontificia Universidad Católica de Chile, Casilla 306, Santiago, Chile*

(Received 3 March 2022; revised 10 April 2022; accepted 11 April 2022; published 25 April 2022)

Auto-oscillations of the magnetization in ferromagnetic hybrid nanostructures driven by spin currents produced by a variety of processes have attracted attention for their challenging physics and possible applications, such as microwave assisted magnetic recording, neuromorphic computing, and chip to chip wireless communications. Of particular interest are applications in which the spin current is produced by a thermal gradient in the configuration of the spin Seebeck effect, because it makes it possible to harvest the thermal energy generated in nanodevices. A few years ago, it was demonstrated experimentally that in a simple bilayer made of a thin film of the insulating ferrimagnet yttrium iron garnet in contact with a platinum layer, the application of a temperature difference across the bilayer produced a coherent microwave auto-oscillation. This device was called a spin caloritronic nano-oscillator. Here we show that these experiments are explained quantitatively by a theory based on a mechanism in which one magnon in the spin current splits into two magnons, one of them being the magnon mode resonating at the nanostructure. The theoretical value of the critical temperature gradient necessary to overcome the magnetic damping to produce auto-oscillations is in good agreement with the one employed in the experiments.

DOI: 10.1103/PhysRevB.105.144429

I. INTRODUCTION

The continuing discoveries of unusual phenomena involving the interplay of charge, spin, and heat currents, keep opening new frontiers in spintronics offering good opportunities for basic research and potential technological applications. The two most studied spintronic phenomena in hybrid structures made of a magnetic insulator (MI) and a normal metal (NM) are the spin-pumping [1–3] and the spin Seebeck effects [4,5]. The spin-pumping effect (SPE) consists of the generation of spin currents by precessing spins in a ferromagnetic layer into an adjacent metal layer with strong spin-orbit scattering [6,7], while the spin Seebeck effect (SSE) refers to the generation of spin currents by thermal gradients in a MI layer [4,5,8–13]. The two most usual manifestations of the SPE are the conversion of the spin current into a charge current in the NM by the inverse spin Hall effect (ISHE) [14–20] and the additional damping of the magnetization in the MI layer due to the angular momentum carried by the spin current through the interface [6,7]. Similarly, the spin current generated in the SSE can be detected either by the charge current created by means of the ISHE along an adjacent NM layer [4,5,8–13] or by the change in the magnetization damping of the MI layer [21–27]. In one remarkable experiment, Safranski and co-workers were able to obtain full compensation of the damping by injecting a thermally generated spin current into the MI layer so as to achieve a spin caloritronic nano-oscillator [27].

The increased damping of a MI layer due to an outflowing spin current produced by microwave-driven SPE has an important reciprocal effect; namely, an inflowing spin current can decrease and even cancel the net damping so as to generate oscillations in the magnetization. The control of the magnetization damping produced by a spin current created by the conversion from a charge current in a NM layer through the spin Hall effect has been observed in many systems [28–38]. In this case, the experimental results are accounted for quantitatively by a model in which the effect of the spin current enters into the Landau-Lifshitz-Gilbert equation in the form of an antidamping spin-transfer torque [34,39,40]. In the case of spin currents generated by a thermal gradient in the SSE flowing out or into a MI, several mechanisms have been proposed for the increase or decrease of the damping. The first mechanism considers that the change originates in the magnon spin current created in the bulk of the MI film by the SSE, which, depending on the sign of the gradient, adds to or subtracts from the spin-pumping current through the interface [41]. The second mechanism is based on the direct action on the magnetization of the antidamping spin-transfer torque created by the spin current generated in the SSE [24]. Another mechanism considers that the magnons are driven by the phonon heat current created by the thermal gradient [42]. Finally, Ref. [43] proposes a mechanism in which the magnon modes of interest are excited by thermally activated magnons in the ferromagnet, driven by a spin Seebeck effect, by means of a three-magnon process, similar to the one in the theory presented here, but with a different magnon interaction. It turns out that, as we show in Sec. II, none of these four mechanisms can explain quantitatively the experimental results.

*sergio.rezende@ufpe.br

In this paper, we present a theory for the spin caloritronic nano-oscillator driven by magnonic spin currents created by thermal gradients in the SSE based on a process in which one magnon in the spin current splits into two magnons. We consider that the magnons in the mode resonating in the nanostructure are driven by magnons in the spin current by means of a three-magnon splitting process mediated by the dipolar interaction, with conservation of energy and momentum. The theoretical value of the negative damping produced by the temperature gradient comfortably explains the damping compensation observed experimentally. In Sec. II we show that previously proposed models for the antidamping mechanisms do not explain quantitatively the experimental results. Sections III and IV are devoted to the formulation of the theory for magnon pumping by the three-magnon splitting process driven by the magnonic spin current. In Sec. V we compare the results of the theory with the temperature gradients used in the experiments of the spin caloritronic nano-oscillator and present the conclusions.

II. CONSIDERATIONS ABOUT PREVIOUSLY PROPOSED MODELS

One model proposed [41] for the control of the magnetic damping in a bilayer made of a ferromagnetic insulator (FMI) in contact with a normal metal (NM) by a thermal gradient relies on the magnonic spin-current theory for the spin Seebeck effect [12,13]. The authors consider a FMI/NM bilayer under microwave driving that excites a coherent magnon with wave number k and frequency ω_k and a thermal gradient across the thickness. They show that the bulk magnon spin current generated through the spin Seebeck effect superimposes to the spin current at the FMI/NM interface created by the magnetization dynamics that produces the spin-pumping damping, so that the total relaxation rate is

$$\eta_T = \eta_k + \frac{\gamma\hbar\omega_k g_{\rm eff}^{\uparrow\downarrow}}{4\pi M t_{\rm FMI}}\left(1 - \frac{\tau_k v_k c_T}{M}\nabla_y T\right), \tag{1}$$

where η_k is the intrinsic coherent magnon relaxation rate, γ is the gyromagnetic ratio, M and $t_{\rm FMI}$ are the FMI magnetization and thickness, $g_{\rm eff}^{\uparrow\downarrow}$ is the spin-mixing conductance of the interface, τ_k and v_k are the coherent magnon relaxation time and velocity, $\nabla_y T = \partial T/\partial y$ is the amplitude of the temperature gradient, and $c_T = -\partial M/\partial T$. The second term in Eq. (1) is the net spin-pumping damping which, depending on the sign of the temperature gradient, can be increased or decreased due to spin current produced by the thermal gradient. Although this result explains quantitatively some experimental observations of the effect of a thermal gradient on the magnon damping in the insulating ferrimagnet yttrium iron garnet (YIG) [25], it cannot account for the full damping compensation necessary for the operation of the spin caloritronic nano-oscillator.

Another mechanism proposed for the control of the magnetic damping by a thermal gradient is based on the concept of spin-transfer torque (STT) [44]. The FMI magnetization dynamics under the action of the STT produced by the spin current $\vec{J}_S$ with polarization $\hat{\sigma}$ created by the SSE is governed by the Landau-Lifshitz-Gilbert equation [24,29],

$$\frac{d\vec{M}}{dt} = \gamma\vec{M}\times\vec{H}_{\rm eff} + \frac{\alpha}{M}\vec{M}\times\frac{d\vec{M}}{dt} - \gamma\frac{J_S}{M^2 t_{\rm FMI}}\vec{M}\times\left(\vec{M}\times\hat{\sigma}\right)\Big|_{\rm int}, \tag{2}$$

where $\vec{H}_{\rm eff}$ is the total effective field acting on the magnetization of the FMI layer with thickness $t_{\rm FMI}$, α is the Gilbert damping parameter, and the last term represents the STT at the interface. Comparison of the last two terms in Eq. (2) shows that the effect of the torque is to change the magnetic relaxation rate by

$$\Delta\eta = -\gamma\frac{J_S}{M t_{\rm FMI}}. \tag{3}$$

In the SSE, the spin current at the FMI/NM interface is proportional to the temperature gradient across the bilayer, $J_S = C_S\nabla_y T$, so that the variation in the relaxation rate due to the thermal gradient is given by

$$\Delta\eta = -\gamma\frac{C_S}{M t_{\rm FMI}}\nabla_y T. \tag{4}$$

The parameter C_S can be obtained directly in a SSE experiment with a FMI/NM bilayer, since the charge-current density J_C measured in the NM layer is related to the spin current by $J_C = \theta_H J_S$. For a YIG/Pt bilayer, using the parameters $C_S = 5\times10^{-10}$ erg/K cm, calculated from the measured SSE voltages [12,13], $M = 144$ G, $t_{\rm FMI} = 23$ nm, and $\gamma = 1.76\times10^7\ {\rm s^{-1}\,Oe^{-1}}$, we obtain for the variation of the relaxation rate due to a thermal gradient,

$$\Delta\eta = -23.5\,\nabla_y T\ {\rm s^{-1}\,K^{-1}\,cm}. \tag{5}$$

This result shows that with a typical gradient of 200 K/cm in a YIG/Pt bilayer, the variation in the damping is only $4.95\times10^3\ {\rm s^{-1}}$, which is much smaller than the magnetic relaxation rate of at least $10^7\ {\rm s^{-1}}$.

The mechanism proposed in Ref. [42] for the magnon instability accompanied by microwave emission in a MI/NM bilayer driven by a temperature gradient is based on the change in the magnon lifetime by the phonon heat current. The authors demonstrate that the magnon instability occurs upon suppression of the umklapp scattering at low temperatures, leading to microwave emission. This mechanism does not explain the experiments of Ref. [27] demonstrating the spin caloritronic nano-oscillator because the experiments were carried out at room temperature. Also, the material used in the MI layer is yttrium iron garnet (YIG), that has a small magnon-phonon interaction. Finally, as mentioned in the Introduction, in the mechanism proposed in Ref. [43], the magnon modes undergoing instability are excited by magnons in the spin current produced in the MI layer in the spin Seebeck effect by means of three-magnon scattering, similarly to the mechanism presented in Sec. III. However, the theory has several ingredients that hinder its ability to explain the spin caloritronic oscillator experiments. First, it considers a three-magnon confluence process, in which two thermally excited magnons are annihilated and one instability magnon is created. Since the driven magnons in the experiments of Ref. [27] have a small wave number and the three-magnon

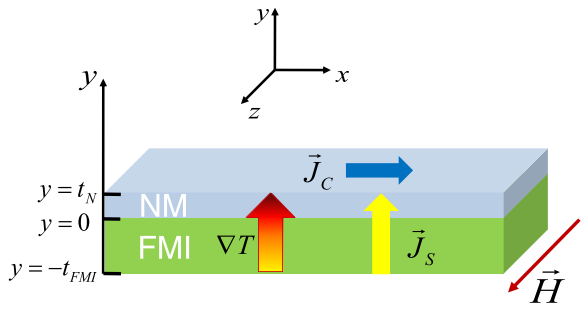

FIG. 1. Illustration of the ferromagnetic insulator (FMI)/normal metal (NM) bilayer and coordinate axes used to formulate the theoretical model for the microwave oscillator produced by the thermally generated magnonic spin current in the configuration of the spin Seebeck effect.

process must conserve energy and momentum, the thermally activated magnon modes in the spin current occupy a very small volume in the center of the Brillouin zone, making the process quite inefficient. The second difficulty of the theory is that it considers the anisotropy energy as the source of the magnon-magnon interaction, and further that the magnetization is misaligned relative to the main crystalline axes so as to break the SU(2) symmetry and produce a torque. It turns out that in YIG the anisotropy field is much smaller than the magnetization, so that the contribution of the anisotropy to the three-magnon scattering is much smaller than the dipolar interaction considered here. In summary, none of the four mechanisms proposed earlier can explain quantitatively the spin caloritronic nano-oscillator experiments of Ref. [27].

III. MAGNONIC SPIN CURRENT GENERATED BY A THERMAL GRADIENT

The mechanism proposed here for the spin caloritronic oscillator involves the magnon flow in the spin current in a ferromagnetic insulator created by a thermal gradient. Thus, in this section, we review the theory for the spin Seebeck effect based on the thermal magnonic spin current [12,13,45]. Initially, we calculate the distribution in configuration space of the magnon distribution in the spin current. Consider the FMI/NM bilayer illustrated in Fig. 1, in the presence of a temperature gradient normal to the plane and with a static magnetic field H applied in the plane. The spin current in the FMI is carried by spin waves (magnons) with wave vector $\vec{k}$ and energy $\hbar\omega_k$. Call n_k the number of magnons with wave number k in the volume V of the FMI layer, n_k^0 the number in thermal equilibrium, given by the Bose-Einstein distribution, $n_k^0 = 1/[\exp(\hbar\omega_k/k_BT) - 1]$, and $\delta n_k = n_k - n_k^0$ the number in excess of equilibrium. The magnon accumulation δn_m, defined as the density of magnons in excess of equilibrium [46,47], is

$$\delta n_m(y) = \frac{1}{(2\pi)^3}\int d^3k\big[n_k(y) - n_k^0\big] = \frac{1}{(2\pi)^3}\int d^3k\delta n_k. \tag{6}$$

The magnon spin-current density with polarization z, $\vec{J}_S^z$, related to the magnetization current $\vec{J}_M^z$ by $\vec{J}_S^z = \vec{J}_M^z/\gamma$, can be written as

$$\vec{J}_S^z(y) = \frac{\hbar}{(2\pi)^3}\int d^3k\vec{v}_k\big[n_k(y) - n_k^0\big], \tag{7}$$

where $\vec{v}_k$ is the k-magnon velocity. The distribution of the magnon number under the influence of a thermal gradient can be calculated with the Boltzmann transport equation (BTE). In the absence of external forces and in the relaxation approximation, in steady state BTE gives

$$n_k(y) - n_k^0 = -\tau_k\vec{v}_k\cdot\nabla n_k(y), \tag{8}$$

where τ_k is the k-magnon relaxation time. Using Eq. (8) in (7) one can show [12,13,45] that the spin current is the sum of two parts, $\vec{J}_S^z = \vec{J}_{S\nabla T}^z + \vec{J}_{S\delta n}^z$, where

$$\vec{J}_{S\nabla T}^z = -\frac{\hbar}{(2\pi)^3}\int d^3k\tau_k\frac{\partial n_k^0}{\partial T}\vec{v}_k(\vec{v}_k\cdot\nabla T) \tag{9}$$

is the contribution of the temperature gradient and

$$\vec{J}_{S\delta n}^z(y) = -\frac{\hbar}{(2\pi)^3}\int d^3k\,\tau_k\,\vec{v}_k[\vec{v}_k\cdot\nabla\delta\,n_k(y)] \tag{10}$$

is due to the spatial distribution of the magnon accumulation. With the temperature gradient ∇T normal to the plane, Eq. (9) gives the spin current in the y direction,

$$J_{S\nabla T}^z = -S_S^z\nabla_y T, \tag{11}$$

$$S_S^z = \frac{\hbar}{(2\pi)^3 T}\int d^3k\tau_k v_{ky}^2\frac{e^x x}{(e^x-1)^2}, \tag{12}$$

where T is the average temperature and $x = \hbar\omega_k/k_BT$ is the normalized magnon energy. Equation (10) represents a spin current due to the spatial variation of the magnon occupation number, so it can be written as a diffusion current,

$$J_{S\delta n}^z(y) = -\hbar D_m\frac{\partial}{\partial y}\delta n_m(y), \tag{13}$$

where D_m is the diffusion parameter to be calculated. Considering the conservation equation,

$$\frac{\partial}{\partial y}J_{S\delta n}^z(y) = -\hbar\frac{\delta n_m(y)}{\tau_{mp}}, \tag{14}$$

where τ_{mp} is the time it takes for the magnon system to relax to the phonon temperature, we have in the steady state a diffusion equation for the magnon accumulation,

$$\frac{\partial^2\delta n_m(y)}{\partial y^2} = \frac{\delta n_m(y)}{l_m^2}, \tag{15}$$

where l_m is the diffusion length, related to the diffusion parameter by $D_m = l_m^2/\tau_{mp}$. The solutions of Eq. (15) can be written as

$$\delta n_m(y) = A\cosh\left[(y + t_{\rm FMI})/l_m\right] + B\sinh\left[(y + t_{\rm FMI})/l_m\right]. \tag{16}$$

Using (16) in Eq. (13) we obtain the total y component of the z-polarized magnon spin-current density in the FMI,

$$J_S^z(y) = -S_S^z \nabla_y T - \hbar \frac{D_m}{l_m} A \sinh\left[(y + t_{\rm FMI})/l_m\right] - \hbar \frac{D_m}{l_m} B \cosh\left[(y + t_{\rm FMI})/l_m\right], \quad (17)$$

where the coefficients A and B are determined by the boundary conditions set by conservation of the angular momentum flow that requires continuity of the spin currents at the FMI/NM interface ($y = 0$), and $J_S^z = 0$ at the substrate/FMI interface ($y = -t_{\rm FMI}$). The spin current is injected into the NM layer by means of the spin pumping produced by the magnetization dynamics associated to the thermal magnon accumulation at the interface [12,13]. Notice that the presence of the NM layer provides a means for the flow of the spin current and is essential for its existence. In spin Seebeck experiments the NM layer is used as a detector of the thermally generated spin current that is converted into a charge current by means of the inverse spin Hall effect. With the boundary conditions, one obtains the relations between the coefficients A and B with the magnon accumulation at the FMI/NM interface and from Eq. (18) one finds the spin-current density at the interface [13,45],

$$J_S(0) = -C_S \nabla_y T, \quad (18)$$

where we have omitted the superscript z for simplicity, and the spin Seebeck coefficient is given by

$$C_S = F \frac{B_1 B_s}{(B_0 B_2)^{1/2}} \rho g_{\rm eff}^{\uparrow\downarrow}, \quad (19)$$

where ρ is a factor that represents the effect of the finite FMI layer thickness, given by

$$\rho = \frac{\cosh(t_{\rm FMI}/l_m) - 1}{\sinh(t_{\rm FMI}/l_m)}, \quad (20)$$

such that $\rho \approx 1$ for $t_{\rm FMI} \gg l_m$ and $\rho \approx 0$ for $t_{\rm FMI} \ll l_m$. The factor F in (19) depends on material parameters and universal constants,

$$F = \frac{\gamma \hbar k_B \tau_{mp}^{1/2} \tau_0^{1/2} k_m^2 \omega_{\rm ZB}}{4\pi M \pi 2\sqrt{3}}, \quad (21)$$

where $\omega_{\rm ZB}$ is the zone boundary magnon frequency, k_m is the value of the maximum wave number assuming a spherical Brillouin zone, τ_0 is the lifetime of magnons near the zone center ($k \approx 0$), and the parameters B in Eq. (19) are given by the integrals

$$B_s = \int_0^1 dq q^2 \sin^2\left(\frac{\pi q}{2}\right) \frac{e^x x}{\eta_q (e^x - 1)^2}, \quad B_1 = \int_0^1 dq q^2 \frac{x^2}{e^x - 1}, \quad (22)$$

$$B_0 = \int_0^1 dq q^2 \frac{x}{e^x - 1}, \quad B_2 = \int_0^1 dq q^2 \sin^2\left(\frac{\pi q}{2}\right) \frac{x}{\eta_q (e^x - 1)}. \quad (23)$$

In Eqs. (22) and (23) $q = k/k_m$ is a normalized wave number and $\eta_q = \eta_k/\eta_0$ is an adimensional relaxation rate. Numerical calculation of these integrals with the magnon dispersion relation for YIG [12]

$$\omega_k = \omega_{\rm ZB}\left(1 - \cos\frac{\pi q}{2}\right), \quad (24)$$

using $\omega_{\rm ZB} = 4.4\times10^{13}\ {\rm s}^{-1}$, $\tau_0 = 0.5\times10^{-7}$ s, and the magnon relaxation rate of Ref. [12] gives $B_s = 0.0002$, $B_0 = 0.617$, $B_1 = 0.23$, and $B_2 = 0.000\,16$. Using in Eqs. (19) and (21) these values, as well as $k_m = 1.74\times10^7\ {\rm cm}^{-1}$, $\tau_{mp} = 10^{-12}$ s, and $g_{\rm eff}^{\uparrow\downarrow} = 10^{14}\ {\rm cm}^{-2}$ for a YIG/Pt bilayer, we obtain for the coefficient of the thermal spin-current density in Eq. (19) $C_S = 4.9\times10^{-8}$ erg/K cm, which is in excellent agreement with the value measured experimentally, used in Sec. II.

A very important quantity for us here is the magnon accumulation in the FMI, given by Eq. (16). With the expressions for the coefficients in (16) calculated with the boundary conditions one can show that the variation with y of the magnon accumulation in the FMI is [12,13]

$$\delta n_m(y) = \frac{l_m C_S \nabla_y T}{\hbar D_m} \left\{ \left[\frac{\rho(t_{\rm FMI}/l_m)}{\sinh(t_{\rm FMI}/l_m)} + \tanh(t_{\rm FMI}/l_m) \right] \cosh\left[(y + t_{\rm FMI})/l_m\right] - \sinh\left[(y + t_{\rm FMI})/l_m\right] \right\}. \quad (25)$$

Using the coefficients in Eq. (18) one obtains for the variation of the spin-current density in the FMI,

$$J_S(y) = -C_S \nabla_y T \{1 + \tanh(t_{\rm FMI}/l_m) \sinh\left[(y + t_{\rm FMI})/l_m\right] - \cosh\left[(y + t_{\rm FMI})/l_m\right] - \tanh\left[(y + t_{\rm FMI})/l_m\right]\}. \quad (26)$$

The variations of the magnon accumulation and spin-current density along the direction perpendicular to the sample plane calculated with Eqs. (25) and (26) for a FMI with $t_{\rm FMI} = l_m$ are shown in Fig. 2.

IV. MECHANISM FOR MAGNON PUMPING BY A MAGNONIC SPIN CURRENT

The mechanism proposed here for driving magnons consists of a three-magnon (3-m) splitting process due to the dipolar interaction, in which one magnon in the magnonic spin current splits into two magnons, one of them being the mode that is in a resonance condition at the sample structure, as illustrated in Fig. 3. This mode has a wave vector determined by the sample shape and dimensions, and frequency that also depends on the applied magnetic field. In samples with nanometric dimensions, the wave number of the resonating magnon mode is on the order of $k \sim 10^6\ {\rm cm}^{-1}$, which is near the center of the Brillouin zone. This mechanism is similar to the one used to explain the pumping of phonons by magnonic spin currents [48]. Considering long wavelength magnons in a cubic ferromagnetic crystal and neglecting the effect of the

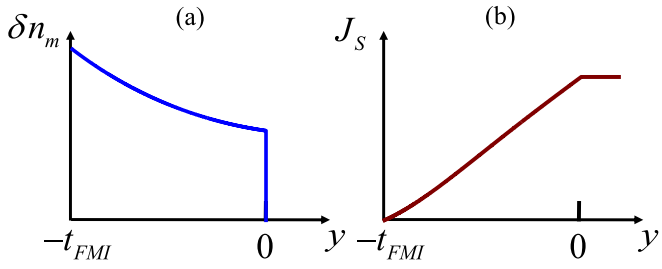

FIG. 2. Variations of the magnon accumulation (a) and spin-current density (b) along the coordinate normal to the sample plane.

surfaces, the dipolar interaction gives for the 3-m Hamiltonian [49–51],

$$H_{dip}^{(3)} \approx -g\mu_B \frac{\pi M}{\sqrt{2SN}} \sum_{k_1,k_2,k} \Delta(\vec{k}_1 - \vec{k}_2 - \vec{k}) \times \left[\left(\sin 2\theta_{k_2} e^{-i\varphi_{k_2}} + \sin 2\theta_k e^{i\varphi_k}\right) c_{k_1}^\dagger c_{k_2} c_k + \text{H.c.}\right], \tag{27}$$

where we have used $M = g\mu_B SN/V$. For the 3-m splitting process we have

$$H_{3m} = \sum_{k_1,k_2,k} \left(V_{3m} c_{k_1}^\dagger c_{k_2}^\dagger c_k + V_{3m}^* c_{k_1} c_{k_2} c_k^\dagger\right) \Delta(\vec{k}_1 - \vec{k}_2 - \vec{k}), \tag{28}$$

where V_{3m} is originated by the dipolar interaction (27). In this process, a magnon with wave vector $\vec{k}_1$ splits into a thermal magnon $\vec{k}_2$ to generate a third magnon $\vec{k}$, conserving momentum and energy. Note that the four-magnon interaction also contributes to the change in the magnon damping. However, the four-magnon interaction arising from the dipolar energy is of higher order compared to Eq. (28) and the one arising from exchange is small for magnon modes in the center of the Brillouin zone [49–51]. Also, the three-magnon interaction arising from the anisotropy energy is nonzero only for the magnetization misaligned with the crystal axes, and in YIG it is much smaller than the dipolar one.

The probability that one magnon of the n_k mode is created in this process can be calculated with first-order perturbation theory. The matrix element that corresponds to this process is, with the Hamiltonian (28),

$$\langle n_{k_1} - 1, n_k + 1, n_{k_2} + 1 | H_{3m} | n_{k_1}, n_k, n_{k_2} \rangle = \left[n_{k_1}(n_k + 1)(n_{k_2} + 1)\right]^{1/2} (V_{3m}). \tag{29}$$

Thus, the probability per unit time for the number of magnons n_k to increase by one unit, given by the Fermi

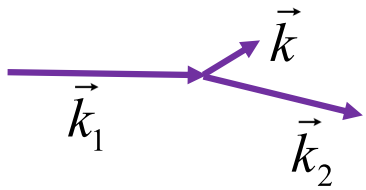

FIG. 3. Illustration of three-magnon splitting process.

"golden rule," is

$$W_{n_k \to n_k+1} = \frac{2\pi}{\hbar^2} \sum_{k_2} (2V_{3m})^2 [n_{k1}(n_k + 1)(n_{k2} + 1)] \times \delta(\omega_{k1} - \omega_k - \omega_{k2}), \tag{30}$$

where the sum runs only over $\vec{k}_2$ because of the momentum conservation relation $\vec{k}_1 = \vec{k} + \vec{k}_2$. The factor 2 is due to the fact that the mode k of interest can be either one of the created pair. The reverse process by which the number of magnons decreases by one unit is calculated in a similar manner, so that the time rate of change of the magnon number is given by

$$\frac{dn_k}{dt} = W_{n_k \to n_k+1} - W_{n_k \to n_k-1}. \tag{31}$$

Thus, we find that the rate of change for the number of magnons in mode $\vec{k}$ to increase by means of the magnon splitting process is

$$\frac{dn_k}{dt} = \frac{2\pi}{\hbar^2} \sum_{k_2} (2V_{3m})^2 [n_{k1}(n_k + 1)(n_{k2} + 1) - n_k n_{k2}(n_{k1} + 1)] \delta(\omega_{k1} - \omega_k - \omega_{k2}). \tag{32}$$

Introducing the excess in the magnon number of the pumping mode 1 and considering that the magnon mode 2 is in thermal equilibrium, omitting the ks in the subscript to simplify the notation, Eq. (32) gives

$$\frac{dn_k}{dt} = \frac{2\pi}{\hbar^2} \sum_{k_2} (2V_{3m})^2 [(n_k + 1)\delta n_1 + \delta n_1 \bar{n}_2 + (n_k + 1) \times \bar{n}_1(\bar{n}_2 + 1) - n_k \bar{n}_2(\bar{n}_1 + 1)] \delta(\omega). \tag{33}$$

In thermal equilibrium $dn_k/dt = 0$, so that we have the following relation for the thermal numbers $(\bar{n}_k+1)\bar{n}_1(\bar{n}_2+1) - \bar{n}_k\bar{n}_2(\bar{n}_1 + 1) = 0$. Actually, this relation follows directly from the expression for the Bose-Einstein distribution. Thus, we can add this null result to Eq. (33), which becomes

$$\frac{dn_k}{dt} = \frac{2\pi}{\hbar^2} \sum_{k_2} (2V_{3m})^2 [(n_k + 1)\delta n_1 + 2\delta n_1 \bar{n}_2 + (n_k - \bar{n}_k)\bar{n}_1(\bar{n}_2 + 1) - (n_k - \bar{n}_k)\bar{n}_2(\bar{n}_1 + 1)] \delta(\omega). \tag{34}$$

Note that if there is no spin-current pumping, $\delta n_1 = 0$ and this equation becomes

$$\frac{dn_k}{dt} = -(n_k - \bar{n}_k) \frac{2\pi}{\hbar^2} \sum_{k_2} (2V_{3m})^2 \times [\bar{n}_2(\bar{n}_1 + 1) - \bar{n}_1(\bar{n}_2 + 1)] \delta(\omega), \tag{35}$$

which is consistent with the equation for the relaxation rate for the three-boson splitting process [49–51]. Since the wave number of the pumped magnon mode in experiments is on the order of $10^6\,\text{cm}^{-1}$ and the magnons involved have a wave number $\sim 10^7\,\text{cm}^{-1}$, we consider that $k_2 = k_1 - k \approx k_1$. We also consider that the magnon mode population n_2 is not perturbed much from thermal equilibrium, so that $n_2 \approx \bar{n}_2$.

Thus, leaving the damping term out, Eq. (35) becomes

$$\frac{dn_k}{dt} = n_k \frac{2\pi}{\hbar^2} \sum_{k_m} (2V_{3m})^2 \delta n_{k2} \delta(\omega_{k1} - \omega_k - \omega_{k2}). \quad (36)$$

This expression can be written in the form

$$\frac{dn_k}{dt} = \alpha_k n_k, \quad (37)$$

where

$$\alpha_k = \frac{8\pi}{\hbar^2} \sum_{k_m} V_{3m}^2 \delta n_{k2} \delta(\omega_{k1} - \omega_k - \omega_{k2}), \quad (38)$$

$$V_{3m} \approx -\gamma \hbar \frac{2\pi M}{\sqrt{2SN}}, \quad (39)$$

showing that the three-magnon interaction can drive the magnon population exponentially in time. In (39) we have used an approximate expression for the vertex of the 3-m interaction neglecting its dependence on the angles of the wave vectors. Thus, the rate of magnon pumping becomes

$$\alpha_k = \frac{16\pi}{\hbar^2} \gamma^2 \hbar^2 \frac{\pi^2 M^2}{SN} \sum_{k_m} \delta n_{k2} \delta(\omega_{k1} - \omega_k - \omega_{k2}). \quad (40)$$

Replacing the sum by an integral in the Brillouin zone, using

$$\frac{1}{N} \sum_k \rightarrow \frac{\Omega}{(2\pi)^3} \int d\vec{k}, \quad (41)$$

we have

$$\alpha_k = \frac{\gamma^2 16\pi^3 M^2}{S} \frac{a^3}{(2\pi)^3} \int d\vec{k}_2 \delta n_{k2} \delta(\omega_{k1} - \omega_k - \omega_{k2}), \quad (42)$$

that has the dimension of time^{-1}, as it should. In order to evaluate the time rate of magnon pumping we need first to calculate the distribution of the relevant magnons in the magnonic spin-current wave vector space. For this, we consider for the magnon number a small deviation from the equilibrium distribution in the form $n_k(\vec{r}) = n_k^0 + n_k^0[1 + \lambda_k g(\vec{r})]$, such that λ_k in the lowest order of energy is chosen so as to eliminate the singularity at $\varepsilon_k = \hbar\omega_k = 0$ [13,45]. This is

$$n_k(\vec{r}) = n_k^0 + n_k^0 \varepsilon_k g(y), \quad (43)$$

where $g(y)$ is a spatial distribution determined by the solution of the boundary-value problem. Substitution in Eq. (6) shows that

$$\delta n_m(y) = I_0 g(y), \quad (44)$$

where $g(y)$ is a function obtained from Eq. (25) and I_0 is a parameter given by the integral

$$I_0 = \frac{1}{(2\pi)^3} \int d^3k n_k^0 \varepsilon_k. \quad (45)$$

Using the relation (44) in (42) we have for the magnon pumping rate,

$$\alpha_k(y) = \delta n_m(y) \frac{\gamma^2 16\pi^3 M^2}{S} \frac{a^3}{(2\pi)^3} \frac{I_\delta}{I_0}, \quad (46)$$

where

$$I_\delta = \frac{1}{(2\pi)^3} \int d\vec{k}_2 n_{k2}^0 \varepsilon_{k2} \delta(\omega_{k1} - \omega_k - \omega_{k2}). \quad (47)$$

The calculation of (47) requires some approximations. First, note that it can be written as

$$I_\delta = \frac{1}{(2\pi)^2} \int k_2^2 dk_2 \int_{-1}^{1} d(\cos\theta_2) n_{k2}^0 \varepsilon_{k2} \delta(\omega_{k1} - \omega_k - \omega_{k2}). \quad (48)$$

Since most contribution to the integral comes from intermediate values of k in the Brillouin zone, we can use the approximate quadratic dispersion relation for magnons [49–51],

$$\omega_k = \gamma[(H + Dk^2)(H + Dk^2 + 4\pi M \sin^2\theta_k)]^{1/2}, \quad (49)$$

where H is the applied magnetic field, D is the exchange parameter, and θ_k is the angle between the wave vector and the field. We can also consider that $H + Dk^2 \gg 4\pi M \sin^2\theta_k$ so that

$$\omega_k \approx \gamma(H + Dk^2 + 2\pi M \sin^2\theta_k). \quad (50)$$

For the evaluation of Eq. (48) we replace the delta function in frequency by

$$\delta(\omega_{k1} - \omega_k - \omega_{k2}) \approx \delta(\omega_{k1} - \omega_{k2}) = \sum_i \frac{\delta(\cos\theta_2 - a_j)}{|d(\omega_{k1} - \omega_{k2})/d\cos\theta_2|}, \quad (51)$$

where a_j are the roots of $(\omega_{k1} - \omega_{k2}) = 0$, given by

$$a_j = \pm\left[\frac{Dk_2^2 - Dk_1^2}{2\pi M} + \cos^2\theta_1\right]^{1/2}. \quad (52)$$

Using momentum conservation $\vec{k}_1 = \vec{k}_2 + \vec{k}$, considering $k_1, k_2 \gg k$, and that the spin current flows perpendicularly to the in-plane field, so that $\theta_1 \approx \pi/2$, one can show that the roots are, approximately, $a_j = \pm(Dk^2/2\pi M)^{1/2}$. Thus, using

$$\frac{d}{d\cos\theta_2}(\omega_{k1} - \omega_{k2}) = \gamma 4\pi M \cos\theta_2, \quad (53)$$

the integral over the angle in Eq. (48) becomes

$$\int_{-1}^{1} d(\cos\theta_2) \delta(\omega_{k1} - \omega_k - \omega_{k2}) = 2[\gamma(8\pi M D k^2)^{1/2}]^{-1}. \quad (54)$$

Using this result in Eq. (48) we obtain

$$I_\delta = \frac{1}{\gamma(8\pi M D)^{1/2} k} I_0, \quad (55)$$

where k is the wave number of the pumped magnon, which is determined by the dimension of the resonating structure in the sample. Equation (46) shows that the time rate of magnon pumping varies in space, because so does the magnon accumulation carried by the spin current. Considering $t_{\mathrm{FMI}} \ll l_m$, Eq. (25) gives a relation between the magnon accumulation and the temperature gradient,

$$\delta n_m(0) = \frac{l_m C_S \nabla_y T}{\hbar D_m}. \quad (56)$$

Finally, using the relations (45), (55), and (56) in Eq. (46) we obtain an expression for the pumping rate in terms of the temperature gradient,

$$\alpha_k = 2g_T \nabla_y T, \tag{57}$$

where

$$g_T = \frac{C_S l_m \omega_M^2 a^2}{16\pi S k \hbar D_m \omega_D}, \tag{58}$$

and the frequency parameters are defined by

$$\omega_M = \gamma 4\pi M, \quad \omega_D = \gamma\left(8\pi M D k_m^2\right)^{1/2}, \tag{59}$$

where $k_m = \pi/a$ is the radius of the spherical Brillouin zone.

In the presence of a magnonic spin-current pumping, the time dependence of the magnon population is

$$n_k(t) = n_k(0) e^{(\alpha_k - 2\eta_k)t}, \tag{60}$$

where η_k is the magnon relaxation rate. Thus, in an experiment with a FMI/NM bilayer sample under a thermal gradient applied perpendicularly to the plane, Eqs. (57) and (60) reveal that if the temperature gradient is increased above the critical value $\nabla_y T_{\rm crit} = \eta_k / g_T$, the magnon population initially with thermal values grows exponentially in time. The magnon mode excited corresponds to a standing spin wave, with wave number k determined by a relevant dimension of the sample, similarly to a laser. The frequency of the excited magnon mode varies with k_0 and with the magnetic field intensity, as in Eq. (49). Note that as the pumped magnon population increases in time, the four-magnon interactions come into play to produce two important consequences. These are the saturation of the pumped magnon population and the induction of quantum coherence in the magnon states, similar to the behavior of a current-driven spin-torque nano-oscillator [52].

V. COMPARISON WITH EXPERIMENTS IN YIG/Pt AND CONCLUSIONS

In order to compare the results of the theory with experiments, we consider a YIG/Pt sample such as the one sketched in Fig. 1, with the dimensions of the sample used by Safransky *et al.* [27]. The sample consists of a YIG strip with thickness 23 nm, lateral width of 350 nm, and 15 μm long, grown on a 0.5 mm thick gadolinium gallium garnet (GGG) substrate, onto which an 8 nm Pt layer is deposited. We use for YIG the following parameters: $4\pi M = 1760$ G, $a = 1.24\times10^{-7}$ cm, $S = 2.5$, $\gamma = 1.76\times10^{7}\,\mathrm{s}^{-1}$, $C_S = 4.9\times10^{-8}$ erg/cm K, $D_m = 6.6\,\mathrm{cm}^2/\mathrm{s}$, $l_m = 10^{-4}$ cm, $D = 5.4\times10^{-9}$ Oe cm^2, $k_m = \pi/a = 2.53\times10^{7}\,\mathrm{cm}^{-1}$, and $k = \pi/d = 1.36\times10^{6}\,\mathrm{cm}^{-1}$, where $d = 23$ nm is the YIG thickness. With these values and the frequency parameters $\omega_D = 3.86\times10^{8}\,\mathrm{s}^{-1}$ and $\omega_M = 3.1\times10^{10}\,\mathrm{s}^{-1}$, calculated with Eq. (59), we obtain with Eq. (58) $g_T = 1.6\times10^{5}\,\mathrm{s}^{-1}\,\mathrm{K}^{-1}$cm. Considering the ferromagnetic resonance linewidth measured in Ref. [27], $\Delta H = 1.6$ Oe, the relaxation rate of the pumped magnon can be taken as $\eta_k = \gamma\,\Delta H = 2.8\times10^{7}\,\mathrm{s}^{-1}$. Thus, the critical temperature gradient necessary to achieve full damping compensation is

$$\nabla_y T_{\rm crit} = \frac{\eta_k}{g_T} = 175\,\mathrm{K/cm}. \tag{61}$$

This value is obtained in a sample with total thickness of 0.5 mm by a temperature difference of only 9 K, similar to the ones used in the experiments of Ref. [27].

In conclusion, we have presented a theoretical formulation for the magnon pumping by thermally induced magnonic spin currents that explains quantitatively the experimental observation of microwave generation in a spin caloritronic nano-oscillator, performed with bilayer samples made of a YIG film strip covered by a platinum layer under a thermal gradient [27]. The thermal gradient produces a magnonic spin current that flows across the thickness of the YIG film and injects magnons into the film. We have shown that a mechanism in which one magnon in the spin current splits into two magnons, one of them being the magnon mode resonating at the nanostructure, can effectively decrease the damping. If the temperature gradient overcomes the magnon damping, magnons with a certain frequency in the microwave range are excited, resulting in an auto-oscillation. The critical temperature gradient calculated with the theory is in good agreement with the values used in the realization of the spin caloritronic nano-oscillator. From a fundamental physics point of view, our results represent an important step in the research of the interconversion of heat and spin degrees of freedom. Our findings also might provide an additional boost in the development of spintronic devices for information and communication technologies.

ACKNOWLEDGMENTS

This research was supported in Brazil by Conselho Nacional de Desenvolvimento Científico e Tecnológico (CNPq), Coordenação de Aperfeiçoamento de Pessoal de Nível Superior (CAPES), Financiadora de Estudos e Projetos (FINEP), and Fundação de Amparo à Ciência e Tecnologia do Estado de Pernambuco (FACEPE), and in Chile by Fondo Nacional de Desarrollo Científico y Tecnológico (FONDECYT) Grant No. 1210641.

[1] Y. Kajiwara, K. Harii, S. Takahashi, J. Ohe, K. Uchida, M. Mizuguchi, H. Umezawa, K. Kawai, K. Ando, K. Takanashi, S. Maekawa, and E. Saitoh, Transmission of electrical signals by spin-wave interconversion in a magnetic insulator, Nature (London) **464**, 262 (2010).

[2] C. W. Sandweg, Y. Kajiwara, K. Ando, E. Saitoh, and B. Hillebrands, Enhancement of the spin pumping efficiency by spin wave mode selection, Appl. Phys. Lett. **97**, 252504 (2010).

[3] L. H. Vilela-Leão, C. Salvador, A. Azevedo, and S. M. Rezende, Unidirectional anisotropy in the spin pumping voltage in

yttrium iron garnet/platinum bilayers, Appl. Phys. Lett. **99**, 102505 (2011).

[4] K. Uchida, J. Xiao, H. Adachi, J. Ohe, S. Takahashi, J. Ieda, T. Ota, Y. Kajiwara, H. Umezawa, H. Kawai, G. E. W. Bauer, S. Maekawa, and E. Saitoh, Spin Seebeck insulator, Nat Mater. **9**, 894 (2010).

[5] K. Uchida, H. Adachi, T. Ota, H. Nakayama, S. Maekawa, and E. Saitoh, Observation of longitudinal spin-Seebeck effect in magnetic insulators, Appl. Phys. Lett. **97**, 172505 (2010).

[6] Y. Tserkovnyak, A. Brataas, and G. E. Bauer, Spin pumping and magnetization dynamics in metallic multilayers, Phys. Rev. B **66**, 224403 (2002).

[7] Y. Tserkovnyak, A. Brataas, G. E. W. Bauer, and B. I. Halperin, Nonlocal magnetization dynamics in ferromagnetic heterostructures, Rev. Mod. Phys. **77**, 1375 (2005).

[8] G. E. W. Bauer, E. Saitoh, and B. J. van Wees, Spin caloritronics, Nat Mater. **11**, 391 (2012).

[9] H. Adachi, K. Uchida, E. Saitoh, and S. Maekawa, Theory of the spin Seebeck effect, Rep. Prog. Phys. **76**, 036501 (2013).

[10] S. R. Boona, R. C. Myers, and J. P. Heremans, Spin caloritronics, Energy Environ. Sci. **7**, 885 (2014).

[11] K. Uchida, M. Ishida, T. Kikkawa, A. Kirihara, T. Murakami, and E. Saitoh, Longitudinal spin Seebeck effect: From fundamentals to applications, J. Phys.: Condens. Matter **26**, 343202 (2014).

[12] S. M. Rezende, R. L. Rodríguez-Suárez, R. O. Cunha, A. R. Rodrigues, F. L. A. Machado, G. A. Fonseca Guerra, J. C. López Ortiz, and A. Azevedo, Magnon spin-current theory for the longitudinal spin-Seebeck effect, Phys. Rev. B **89**, 014416 (2014).

[13] S. M. Rezende, R. L. Rodríguez-Suárez, J. C. López Ortiz, and A. Azevedo, Bulk magnon spin current theory for the longitudinal spin Seebeck effect, J. Magn. Magn. Mater. **400**, 171 (2016).

[14] A. Azevedo, L. H. Vilela-Leão, R. L. Rodríguez-Suárez, A. B. Oliveira, and S. M. Rezende, Dc effect in ferromagnetic resonance: Evidence of the spin-pumping effect? J. Appl. Phys. **97**, 10C715 (2005).

[15] E. Saitoh, M. Ueda, H. Miyajima, and G. Tatara, Conversion of spin current into charge current at room temperature: Inverse spin-Hall effect, Appl. Phys. Lett. **88**, 182509 (2006).

[16] O. Mosendz, J. E. Pearson, F. Y. Fradin, G. E. W. Bauer, S. D. Bader, and A. Hoffmann, Detection and Quantification of Inverse Spin Hall Effect from Spin Pumping in Permalloy/Normal Metal Bilayers, Phys. Rev. Lett. **104**, 046601 (2010).

[17] K. Ando, J. I. Takahashi, Y. Kajiwara, H. Nakayama, T. Yoshino, K. Harii, Y. Fujikawa, M. Matsuo, S. Maekawa, and E. Saitoh, Inverse spin-Hall effect induced by spin pumping in metallic system, J. Appl. Phys. **109**, 103913 (2011).

[18] A. Azevedo, L. H. Vilela-Leão, R. L. Rodríguez-Suárez, A. F. Lacerda Santos, and S. M. Rezende, Spin pumping and anisotropic magnetoresistance voltages in magnetic bilayers: Theory and experiment, Phys. Rev. B **83**, 144402 (2011).

[19] A. Hoffmann, Spin Hall effects in metals, IEEE Trans. Magn. **49**, 5172 (2013).

[20] J. Sinova, S. O. Valenzuela, J. Wunderlich, C. H. Back, and T. Jungwirth, Spin Hall effects, Rev. Mod. Phys. **87**, 1213 (2015).

[21] E. Padrón-Hernández, A. Azevedo, and S. M. Rezende, Amplification of Spin Waves by Thermal Spin-Transfer Torque, Phys. Rev. Lett. **107**, 197203 (2011).

[22] L. Lu, Y. Sun, M. Jantz, and M. Wu, Control of Ferromagnetic Relaxation in Magnetic Thin Films through Thermally Induced Interfacial Spin Transfer, Phys. Rev. Lett. **108**, 257202 (2012).

[23] G. L. da Silva, L. H. Vilela-Leão, S. M. Rezende, and A. Azevedo, Enhancement of spin wave excitation by spin currents due to thermal gradient and spin pumping in yttrium iron garnet/Pt, Appl. Phys. Lett. **102**, 012401 (2013).

[24] M. B. Jungfleisch, T. An, K. Ando, Y. Kajiwara, K. Uchida, B. I. Vasyuchka, A. V. Chumak, A. A. Serga, E. Saitoh, and B. Hillebrands, Heat-induced damping modification in yttrium iron garnet/platinum hetero-structures, Appl. Phys. Lett. **102**, 062417 (2013).

[25] R. O. Cunha, E. Padrón-Hernández, A. Azevedo, and S. M. Rezende, Controlling the relaxation of propagating spin waves in yttrium iron garnet/Pt bilayers with thermal gradients, Phys. Rev. B **87**, 184401 (2013).

[26] H. Yu, S. D. Brechet, P. Che, F. A. Vetro, M. Collet, S. Tu, Y. G. Zhang, Y. Zhang, T. Stueckler, L. Wang, H. Cui, D. Wang, C. Zhao, P. Bortolotti, A. Anane, J-Ph. Ansermet, and W. Zhao, Thermal spin torques in magnetic insulators, Phys. Rev. B **95**, 104432 (2017).

[27] C. Safranski, I. Barsukov, H. K. Lee, T. Schneider, A. A. Jara, A. Smith, H. Chang, K. Lenz, J. Lindner, Y. Tserkovnyak, M. Wu, and I. N. Krivorotov, Spin caloritronic nano-oscillator, Nat. Commun. **8**, 117 (2017).

[28] E. Padrón-Hernández, A. Azevedo, and S. M. Rezende, Amplification of spin waves in yttrium iron garnet films through the spin Hall effect, Appl. Phys. Lett. **99**, 192511 (2011).

[29] V. E. Demidov, S. Urazhdin, H. Ulrichs, V. Tiberkevich, A. Slavin, D. Baither, G. Schmitz, and S. O. Demokritov, Magnetic nano-oscillator driven by pure spin current, Nat. Mater. **11**, 1028 (2012).

[30] R. H. Liu, W. L. Lim, and S. Urazhdin, Spectral Characteristics of the Microwave Emission by the Spin Hall Nano-Oscillator, Phys. Rev. Lett. **110**, 147601 (2013).

[31] S. Urazhdin, V. E. Demidov, H. Ulrichs, T. Kendziorczyk, T. Kuhn, J. Leuthold, G. Wilde, and S. O. Demokritov, Nanomagnonic devices based on the spin-transfer torque, Nat. Nanotechnol. **9**, 509 (2014).

[32] V. E. Demidov, S. Urazhdin, B. Divinskiy, A. B. Rinkevich, and S. O. Demokritov, Spectral linewidth of spin-current nano-oscillators driven by nonlocal spin injection, Appl. Phys. Lett. **107**, 202402 (2015).

[33] M. Madami, E. Iacocca, S. Sani, G. Gubbiotti, S. Tacchi, R. K. Dumas, J. Akerman, and G. Carlotti, Propagating spin waves excited by spin-transfer torque: A combined electrical and optical study, Phys. Rev. B **92**, 024403 (2015).

[34] V. Lauer, D. A. Bozhko, T. Brächer, P. Pirro, V. I. Vasyuchka, A. A. Serga, M. B. Jungfleisch, M. Agrawal, Yu. V. Kobljanskyj, G. A. Melkov, C. Dubs, B. Hillebrands, and A. V. Chumak, Spin-transfer torque based damping control of parametrically excited spin waves in a magnetic insulator, Appl. Phys. Lett. **108**, 012402 (2016).

[35] V. E. Demidov, S. Urazhdin, R. Liu, B. Divinskiy, A. Telegin, and S. O. Demokritov, Excitation of coherent propagating spin waves by pure spin currents, Nat. Commun. **7**, 10446 (2016).

[36] M. Evelt, C. Safranski, M. Aldosary, V. E. Demidov, I. Barsukov, A. P. Nosov, A. B. Rinkevich, K. Sobotkiewich, X. Li, J. Shi, I. N. Krivorotov, and S. O. Demokritov, Spin Hall-induced auto-oscillations in ultrathin YIG grown on Pt, Sci. Rep. **8**, 1269 (2018).

[37] J.-R. Chen, A. Smith, E. A. Montoya, J. G. Lu, and I. N. Krivorotov, Spin–orbit torque nano-oscillator with giant magnetoresistance readout, Commun. Phys. **3**, 187 (2020).

[38] J. Holanda, H. Saglam, V. Karakas, Z. Zang, Y. Li, R. Divan, Y. Liu, O. Ozatay, V. Novosad, J. E. Pearson, and A. Hoffmann, Magnetic Damping Modulation in $IrMn_3/Ni_{80}Fe_{20}$ via the Magnetic Spin Hall Effect, Phys. Rev. Lett. **124**, 087204 (2020).

[39] J. Holanda, D. S. Maior, O. Alves Santos, A. Azevedo, and S. M. Rezende, Evidence of phonon pumping by magnonic spin currents, Appl. Phys. Lett. **118**, 022409 (2021).

[40] Y. Zhou, H.-J. Jiao, Y.-T. Chen, G. E. W. Bauer, and J. Xiao, Current-induced spin-wave excitation in Pt/YIG bilayer, Phys. Rev. B **88**, 184403 (2013).

[41] S. M. Rezende, R. L. Rodríguez-Suárez, and A. Azevedo, Thermal control of the spin pumping damping in ferromagnetic/normal metal interfaces, Phys. Rev. B **89**, 094423 (2014).

[42] Y. Ohnuma, H. Adachi, E. Saitoh, and S. Maekawa, Magnon instability driven by heat current in magnetic bilayers, Phys. Rev. B **92**, 224404 (2015).

[43] S. A. Bender and Y. Tserkovnyak, Thermally driven spin torques in layered magnetic insulators, Phys. Rev. B **93**, 064418 (2016).

[44] J. C. Slonczewski, Current-driven excitation of magnetic multilayers, J. Magn. Magn. Mater. **159**, L1 (1996).

[45] S. M. Rezende, R. L. Rodríguez-Suárez, and A. Azevedo, Magnon diffusion theory for the spin Seebeck effect in ferromagnetic and antiferromagnetic insulators, J. Phys. D: Appl. Phys. **51**, 174004 (2018).

[46] S. S.-L. Zhang and S. Zhang, Magnon Mediated Electric Current Drag across a Ferromagnetic Insulator Layer, Phys. Rev. Lett. **109**, 096603 (2012).

[47] S. S.-L. Zhang and S. Zhang, Spin convertance at magnetic interfaces, Phys. Rev. B **86**, 214424 (2012).

[48] S. M. Rezende, D. S. Maior, O. Alves Santos, and J. Holanda, Theory for phonon pumping by magnonic spin currents, Phys. Rev. B. **103**, 144430 (2021).

[49] M. Sparks, *Ferromagnetic Relaxation* (McGraw-Hill, New York, 1964).

[50] R. M. White, *Quantum Theory of Magnetism*, 3rd ed. (Springer-Verlag, Berlin, 2007).

[51] S. M. Rezende, Fundamentals of Magnonics, *Lecture Notes in Physics Vol. 969* (Springer, Cham, 2020).

[52] S. M. Rezende, Quantum coherence in spin-torque nano-oscillators, Phys. Rev. B **81**, 092401 (2010).